

REPORT DOCUMENTATION PAGE

Form Approved OMB No. 0704-0188

Public reporting burden for this collection of information is estimated to average 1 hour per response, including the time for reviewing instructions, searching existing data sources, gathering and maintaining the data needed, and completing and reviewing the collection of information. Send comments regarding this burden estimate or any other aspect of this collection of information, including suggestions for reducing the burden, to Department of Defense, Washington Headquarters Services, Directorate for Information Operations and Reports (0704-0188), 1215 Jefferson Davis Highway, Suite 1204, Arlington, VA 22202-4302. Respondents should be aware that notwithstanding any other provision of law, no person shall be subject to any penalty for failing to comply with a collection of information if it does not display a currently valid OMB control number.
PLEASE DO NOT RETURN YOUR FORM TO THE ABOVE ADDRESS.

1. REPORT DATE (DD-MM-YYYY) 26-01-2006	2. REPORT TYPE Final Report	3. DATES COVERED (From – To) 13 July 2005 - 21-Jun-06
--	---------------------------------------	---

4. TITLE AND SUBTITLE Microstructure of Conventional and Reduced Sensitivity RDX	5a. CONTRACT NUMBER FA8655-05-1-3029
	5b. GRANT NUMBER
	5c. PROGRAM ELEMENT NUMBER

6. AUTHOR(S) Dr. Michael J Herrmann	5d. PROJECT NUMBER
	5d. TASK NUMBER
	5e. WORK UNIT NUMBER

7. PERFORMING ORGANIZATION NAME(S) AND ADDRESS(ES) Fraunhofer Institute for Chemical Technology J.-v.-Fraunhoferstraße 7 Pfinztal 76327 Germany	8. PERFORMING ORGANIZATION REPORT NUMBER N/A
--	--

9. SPONSORING/MONITORING AGENCY NAME(S) AND ADDRESS(ES) EOARD PSC 821 BOX 14 FPO 09421-0014	10. SPONSOR/MONITOR'S ACRONYM(S)
	11. SPONSOR/MONITOR'S REPORT NUMBER(S) Grant 05-3029

12. DISTRIBUTION/AVAILABILITY STATEMENT
Approved for public release; distribution is unlimited.

13. SUPPLEMENTARY NOTES

14. ABSTRACT

This report results from a contract tasking Fraunhofer Institute for Chemical Technology as follows: Reduced Sensitivity (RS) energetic materials are in the scope of interest, particularly, for the development and refinement of IM PBX as PBXN-109. Such improved versions of current explosive ingredients as RDX and HMX facilitate progress in times of limited funding, as an introduction of new ingredients as FOX-7 would give rise to considerably higher costs. However, the mechanisms behind the sensitivity reduction are far from being clear. Particle size, shape, surface morphology, voids, inclusions and impurities, lattice dislocations and deformation twinning of ingredients as RDX and HMX have been discussed to influence the mechanical sensitivity. Within the last years, X-ray diffraction methods have been elaborated and refined at ICT, particularly, for investigating micro strain in energetic materials. These methods shall now be tested for characterizing and distinguishing reduced sensitivity from conventional RDX. A sample portfolio of different crystal qualities of RDX will be collected, including conventional and reduced sensitivity samples, and the samples will be investigated with advanced X-ray diffraction techniques.

15. SUBJECT TERMS
EOARD, Energetic Materials, Explosives, Insensitive Munitions

16. SECURITY CLASSIFICATION OF:			17. LIMITATION OF ABSTRACT UL	18. NUMBER OF PAGES 18	19a. NAME OF RESPONSIBLE PERSON JOAN FULLER
a. REPORT UNCLAS	b. ABSTRACT UNCLAS	c. THIS PAGE UNCLAS			19b. TELEPHONE NUMBER (Include area code) +44 (0)20 7514 3154

Microstructure of Conventional and Reduced Sensitivity RDX

Final Report

by

Dr. Michael Herrmann and Bastian Ludwig
December 2005

EUROPEAN OFFICE OF AEROSPACE RESEARCH AND DEVELOPMENT
London, England
Contract Number: FA8655-05-1-3029
July to December 2005

Contractor:
Fraunhofer Institut für Chemische Technologie
J.-v.-Fraunhofer-Straße 7
76327 Pfinztal / Germany
Principal Investigator: Dr. Michael Herrmann

approved for public release, distribution unlimited

The Research reported in this document has been made possible through the support and sponsorship of the U.S. Government through its European Office of Aerospace Research and Development

List of keywords

Reduced sensitivity, Insensitive, RDX, micro strain, X-ray diffraction

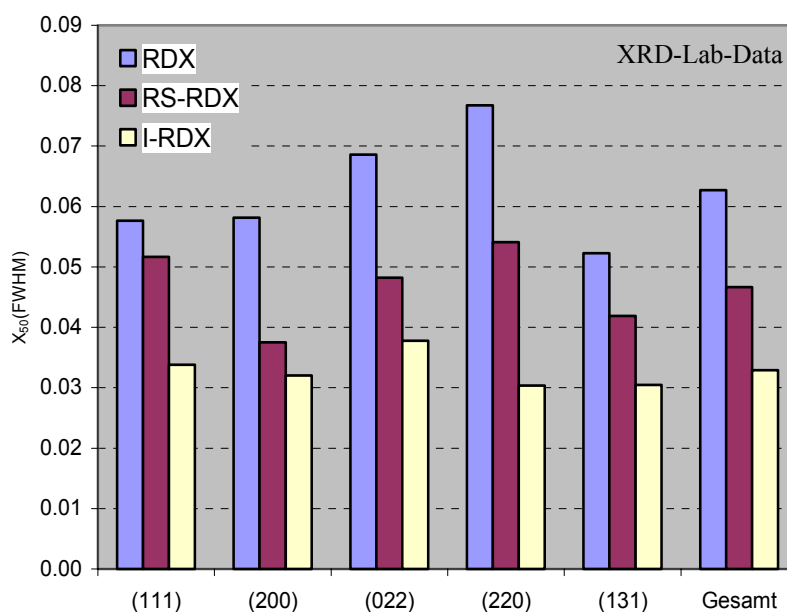
Summary

Reduced Sensitivity (RS) or Insensitive (I) RDX may open the door to improved IM products. Consequently, actual research activities aim on elaboration of broadly feasible methods for distinguishing conventional from reduced sensitive products, at a crystalline level, and on the development of an upgrade version of STANAG 4002 including RS-RDX (NIMIC 2003). X-Ray diffraction (XRD) may provide a powerful tool for these tasks based on peak broadening due to crystallite size and micro strain.

Therefore XRD measurements of RDX, RS-RDX and I-RDX; coarse and fine grades (Class 1 and 5) were performed. Different diffraction techniques have been refined, taking into account the relatively low absorbance of RDX, and particularly the coarse grades of class 1, not suitable for standard XRD measurements. Preparation of samples as thin particle layer reduces penetration depths and peak broadening, but the procedure is still makeshift and thus may impact reproducibility. An alternative technique uses parallel beam geometry, preventing peak broadening due to penetration depth, mean density or uneven sample surface. The combination of this technique with the high flux and resolution of the synchrotron radiation at ANKA delivered best results for class 5 samples.

Rocking curves invert the lack of poor orientation statistics of coarse class 1 powders into an advantage obtaining information from a large number of isolated crystal domains, which are evaluated statistically. The method is very promising, as applicable for as crystallized coarse products.

The investigations reveal significantly different crystal qualities of RDX, RS-RDX and I-RDX by means of X-ray diffraction peak broadening. Poorer crystal quality was found with the conventional RDX compared to RS- and I-RDX for classes 1 and 5. For the coarse class 1 samples significant differences were also found between RS- and I-RDX pointing to a higher crystal quality of I-RDX. The results shall be discussed in terms of micro structure and support development and quality assessment of reduced sensitivity product.



Median peak widths obtained from rocking curves; plot distinguishes conventional from RS- and I-RDX, class 1

Introduction and Objectives

Reduced Sensitivity (RS) energetic materials are in the scope of actual research. The interest stems from investigations showing that careful processing of crystalline energetic ingredients improves the shock sensitivity of plastic bonded explosives as PBXN-109. The effect facilitates progress of Insensitive Munitions development in times of limited funding. Consequently, RS-RDX is used in formulations (HBU-88A and B2213S) and has been considered for numerous other systems, including the US Army 120 mm mortar program. Concomitantly, actual research activities aim on the elaboration of broadly feasible methods for distinguishing conventional from reduced sensitive products, at a crystalline level, and on the development of an upgrade version of STANAG 4002 including RS-RDX (NIMIC 2003). However, the mechanisms behind the sensitivity reduction are far from being clear. Particle size, shape, surface morphology, voids, inclusions and impurities, lattice dislocations and deformation twinning of ingredients as RDX and HMX are discussed to influence the mechanical sensitivity.

Compared to other methods X-ray diffraction allows the characterization and quantitative determination of crystal defects measured not only from the surface and with point measurements but from a representative volume of the substance. The method is based on the broadening of diffraction peaks by lattice defects and related micro strain. It was elaborated by Warren and Averbach and refined by later authors. Within the last years, including EOARD project FA8655-02-M4066 'Characterization of the Microstructure of fine Energetic Materials' (Herrmann 2003), at ICT X-ray diffraction methods has been elaborated and refined, particularly, for the investigation of micro strain in lowly absorbing energetic materials (Herrmann 2005). These methods are now tested for distinguishing reduced sensitivity from conventional RDX.

Most obvious military advantage is expected from providing sophisticated X-ray diffraction analyses for internal crystal quality of energetic materials for quality assessment of RS and IM products and further developments based on a detailed knowledge about structural mechanisms. Besides, the project gains from additional investigations of energetic materials at the synchrotron Karlsruhe ANKA, performed outside this project.

RDX and Sample Portfolio

A sample Portfolio has been collected including different qualities of RDX including conventional and so called Reduced Sensitivity and Insensitive RDX. Samples, medium particle size (X50) and water content are summarized in Tab. 1.

Tab. 1: RDX samples, particle size and water content

ID	Sample	x50 [μm]	water content [%]
Quartz SRM 660a	Quartz Lanthanum hexaboride	20.3 8.78	
RDX C1	RDX, Type I, Class 1	194.54	<0.01
RDX C5	RDX, Type I, Class 5	17.57	0.02
RS-RDX C5	RS-RDX, Type I, Class 5	9.71	0.02
RS-RDX C1	RS-RDX, Type I, Class 1	205.18	<0.01
I-RDX C1	i-RDX CL1	225.36	<0.01
I-RDX M3C	i-RDX M3C	10.51	<0.01

Measuring techniques and Experimental

Diffraction patterns were measured with a diffractometer D5000 from Bruker AXS, equipped with copper tube, vertical soller slits, Ni-k β -filter, rotating sample holder and scintillation counter. Tab. 2 and Tab 5 (Appendix) summarize the instrumental parameters and the diffraction experiments and conditions, respectively. The measurements are designated by X followed by a number e.g. X3; they will be referred by these numbers.

Tab. 2: Instrumental parameters

Goniometer Radii	Value	Full Axial Model	Value
Primary Radius (mm)	217.5	Source Length (mm)	12
Secondary Radius (mm)	217.5	Source Width (mm)	0.04
Equatorial		RS Length (mm)	12
Detector slit (mm)	0.1	Prim. Soller (°)	2.3
FDS Angle (°)	0.5*	Sec. Soller (°)	2.3

New sample holders and preparation techniques

Two sample holders, proposed for measurements with reduced underground, were purchased from Bruker AXS. The holders consist of single silicon crystals embedded in PMMA rings; one with a flat plane, the other with a recess of \varnothing 20 mm x 0.5 mm. Besides, a conventional sample holder has been used, consisting of a plastic holder with a recess of \varnothing 26 mm x 2 mm. The sample holders fit into the spinning devices of the Bragg Brentano Goniometers D5000 or D8. Preparations of samples are performed as follows:

- Standard: recesses single crystal or conventional sample holder is filled up to the edge with powder and the sample surface is flattened with a glass plate.
- Particle layer: small amounts of powders are mixed with distilled water and spread over the flat holder with a spatula. The water could be removed by evaporation or contacting sample area carefully at the rim with a tissue.

The sample holders were tested measuring quartz (X1-X9), varying divergence slit between 0.1 and 0.8 ° and with a compared to 40 kV reduced tube voltage of 30 KV; the voltage reduction is recommended by Bruker AXS for background reduction.

Standard Bragg-Brentano measurements and thin particle layer technique

Diffraction patterns of the RDX samples have been measured with the reduced voltage of 30 KV and the single crystal sample holders. Measurements were performed between 12 and 33 °2 θ with step widths and time per step of 0.005 °2 θ and 6 s (X10-X15) and 0.02 °2 θ and 10 s (X20-X58). The investigations include conventional preparation and thin particle layers. For testing reproducibility of the investigation techniques a coarse and a fine sample, RS-RDX C1 and RS-RDX C5, have been measured five to ten times each with flat and recessed sample holder (X20-X39). Four measurements of each sample with each holder have been performed without sample exchange; materials were only stirred for change orientation of crystals (X21-X25, X26-X29, X36-X39 and X41-X44). The other measurements were performed with new sample material, freshly prepared. Besides, particle layers have been prepared with varying sample quantities (X30-X34 and X45-X48).

For calibration and determining the geometrical profiles the standard reference material SRM 660a from the National Institute of Standards and Technology (NIST 2000) was measured under resembling conditions (X16-19). This line position and shape standard is recommended for size-strain

investigations. It consists of a fine Lanthanum Hexaboride powder with crystallite aggregates in the 2 to 5 μm range.

Rocking curve for coarse powders

Measurements of coarse powders by standard techniques using Bragg Brentano Geometry suffer from poor orientation statistics of crystals; oddly shaped “peaks” hinder a proper profile analysis. Grinding samples below particle sizes of about 10 μm would overcome this problem but would also change the internal crystal quality, to be investigated. Therefore so called rocking curves have been tested for investigation of coarse powders.

Within a rocking curve, radiation source and detector are positioned within a diffraction condition of the sample; which means that the angle 2θ between incident and diffracted beam meets the Bragg law $\lambda = 2d\sin\theta$ for a selected lattice plane distance d_{hkl} of the structure. Now, the sample is turned with an angle $\Delta\theta$ around the symmetric position θ while source and detector are kept fix. With this motion of the sample lattice planes of crystallites are turned into diffraction condition and out again. The method was described e.g. by Schneider 1974 for the investigation of mosaicity of single crystals and was refined for quantification of dislocation densities of powders e.g. by Yaziki et al. 1983.

Measurements X59-X67 were performed at reflection conditions of net planes (111), (200), (022), (220) and (131), with turning the sample holder from -5 to $5^\circ\Delta\theta$ with 0.005° step width and 6 s step time, where $\Delta\theta$ is the tilt of the sample out of the symmetric position. 2θ and θ values are summarized in Tab 5. As patterns shall include reflections from a representative quantity of crystals, on one hand, but without much superposition or overlap hindering a proper evaluation, on the other hand, the rocking curves have been measured with the flat specimen using varying but rather small sample quantities. Coarse RDX and I-RDX was measured twice, RS-RDX even 5 times.

Synchrotron

Beside this work, investigations have been performed at the Angstroem-Source Karlsruhe ANKA. The measurements include a variety of samples, pharmaceuticals, energetic materials, polymers, metals, particularly the RDX samples investigated within this work. Therefore RDX related results of the investigations at ANKA shall be discussed within this work, but details of the investigation at the synchrotron are (Herrmann 2005) and will be reported elsewhere.

Theory and Evaluation

Peak profile analysis of standard measurements and Williamson Hall plot

The diffraction profiles measured with the standard Bragg-Brentano geometry were fitted using the split-Pearson VII (SPVII) analytical function of program TOPAS 2.1 from Bruker AXS, yielding intensity and Full Widths at Half Maximum (FWHM). The FWHM of peaks (111), (200), (002), (021), (102), (229), (221), (131) (322) and (420) were reduced by geometric peak widths obtained from the standard measurements (X16, X17). These peaks have been identified as not significantly interfered by overlap or superposition (Herrmann 2003). Resulting “peak widths of pure sample” were evaluated in terms of reciprocal units as described by Williamson and Hall in 1953 (see highlighted box).

The reciprocal peak widths $\beta^* = \beta \cos\theta/\lambda$ were plotted versus reciprocal lattice distances $d^* = 2\sin\theta/\lambda$, linear regression lines were fitted and their slopes were discussed in terms of micro strain.

Williamson and Hall (1953) suggested that the full width at half-maximum (FWHM) of diffraction profiles can be written as the sum of strain and size broadening, which means in terms of reciprocal units: $\beta^* = \Delta K = 0.9/D + \Delta K^D$ where ΔK^D is the strain contribution to peak broadening and D is the average grain size. ($d^* = K = 2 \sin\theta/\lambda$, $\Delta K = 2 \cos\theta (\Delta\theta)/\lambda$ with the peak width β , the lattice spacing d , the diffraction angle θ , the half of FWHM $\Delta\theta$ and the wave length λ)

The method solves the problem of the separation of size and strain broadening revealing the root mean-squared strain $\langle \varepsilon^2 \rangle^{1/2}$ (Ungar et al. 2000). The root mean squared strain could be estimated according to

$$\eta_\beta = 2\beta^*/d^* \approx 5\langle \varepsilon^2 \rangle^{1/2}$$

with the apparent strain η_β (Langford 2000).

Peak profile analysis of rocking curves

From the average peak widths of rocking curves dislocation may be estimated as described by Spieß or Yaziki (see highlighted box).

The diffraction profiles of the rocking curves were fitted using the symmetric Pearson VII analytical function, yielding the intensity and Full Widths at Half Maximum (FWHM). In contrast to the standard measurements $K_{\alpha 2}$ -part of the emission profile has been removed, as no systematic shoulders appear in the rocking curve patterns. The obtained data were evaluated by plotting normalized additive peak number versus peak widths and by determining median peak widths X_{50} and slopes around this value approximated by X_{25}/X_{75} .

Spieß et al. 2005 describes the Full Width at Half Maximum FWHM β_{rock} of a rocking curve as

$$\beta_{rock}^2 = \beta_{int}^2 + \beta_G^2 + \beta_M^2 + \beta_\varepsilon^2 + \beta_D^2 + \beta_r^2$$

with the intrinsic half width labeled with *int* and the contributions from measuring device G , mosaicity M , micro strain ε , crystallite size D and sample bend r . Of particular interest for the internal crystal quality are the terms for crystallite size, mosaicity and micro strain. The dislocations expected in RDX can contribute to all these terms as

- dislocations tilt net planes, and as parts of small angle grain boundaries tilt neighboring domains. The tilt of coherently diffracting areas (domains) is the characteristic feature of rocking curve broadening due to mosaicity β_M .
- dislocations strain a crystal lattice locally. Subsequent variation of lattice distances broadens rocking curve term β_ε .
- dislocations separate coherently diffracting areas (domains). Small domains broaden rocking curve term β_D .

The mosaicity and micro strain terms may be evaluated according to

$$\beta_M^2 = 2\pi \ln(2) \cdot b^2 \cdot \rho_V$$

$$\beta_\varepsilon^2 = \left[8 \cdot \ln 2 \left(\overline{\varepsilon_N^2} \right) \right] \tan^2 \theta$$

with ρ_V the dislocation density, b the magnitude of Burger vector and the mean square strain $\overline{\varepsilon_N^2}$. (Yaziki reported $D = \beta^2 / 9b^2$ for calculation of excess dislocation density)

Results

Sample holders and preparation techniques

Results of quartz measurements with varying slit widths and sample holders are summarized in Fig. 1 to Fig. 3. The plots show that diffraction peaks are shifted systematically in dependence of the sample holder. Compared to the conventional sample holder (red curves in Fig. 1) peaks are shifted to lower angles with the silicon sample holder with recess (green), but to higher angles with the flat silicon sample holder (blue). Besides, the characteristic of the $K\alpha_1/\alpha_2$ -duplet is carved out clearer when samples have been prepared as thin particle layer on the flat single crystal sample holder (blue), indicating a higher peak resolution. The peak resolution could be further improved by reducing divergence slit width, as shown in Fig. 2, but at the expense of intensity. The results of peak profile analysis of these measurements are summarized in Fig. 3, where FWHM and intensity are plotted versus divergence slit width.

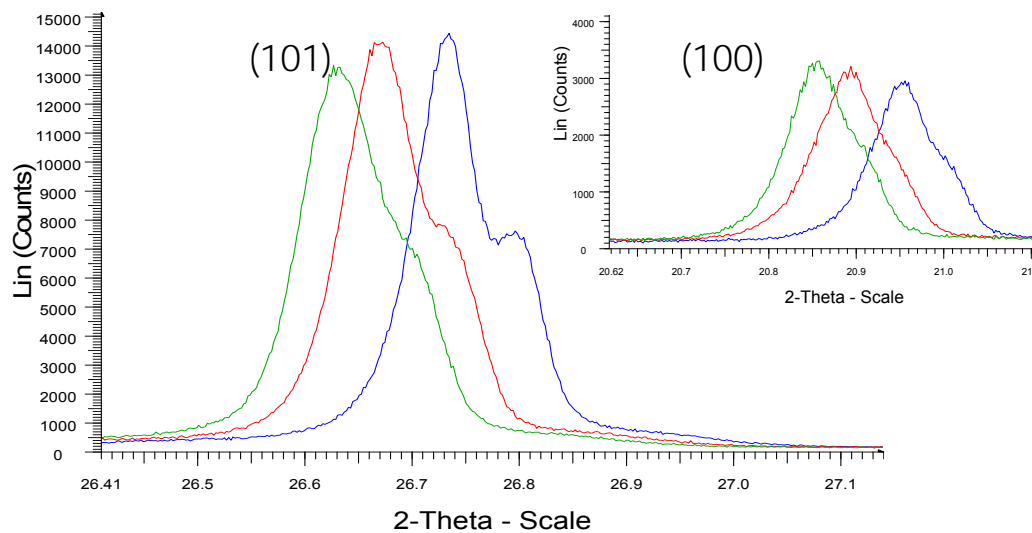


Fig. 1: Comparison of quartz peaks (100) and (101) measured with conventional sample holder (red), recessed (green) and flat silicon sample holder (X1-X3)

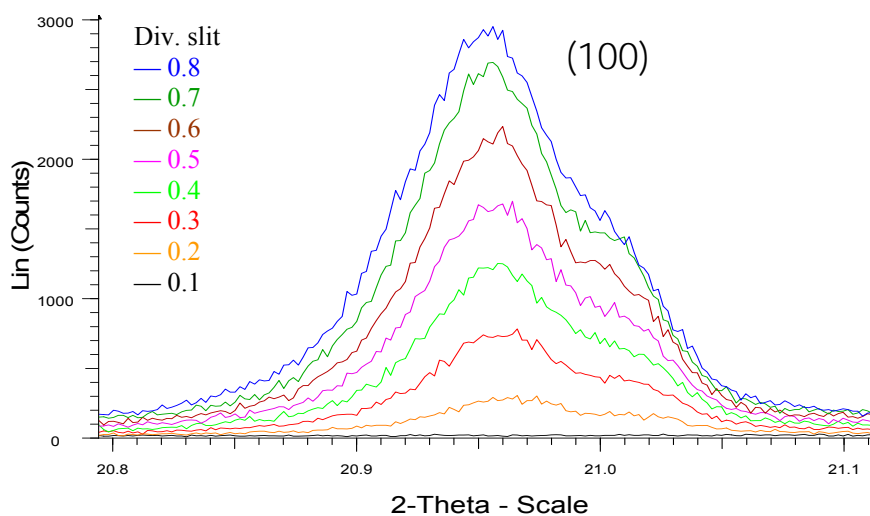


Fig. 2: Quartz peak (101) measured with sample slits varying from 0.1 to 0.8 ° (with recess, X2)

The plots reveal significantly narrower diffraction peaks obtained with the particle layer on the flat silicon single crystal, compared with the conventional and the recessed sample holder. As with smaller values of the divergence slit width the intensity slows down, a medium slit width of 0.5° has been chosen for the subsequent investigations. This value seems to compromise reasonable resolution and intensity.

Using the single crystal sample holders reduced the underground as shown in Fig. 4. Further reduced undergrounds were measured with the lower tube voltage of 30 KV. The reduction was found to be most pronounced with the conventional sample holder; the resulting backgrounds measured with 30 KV were found to resemble one another.

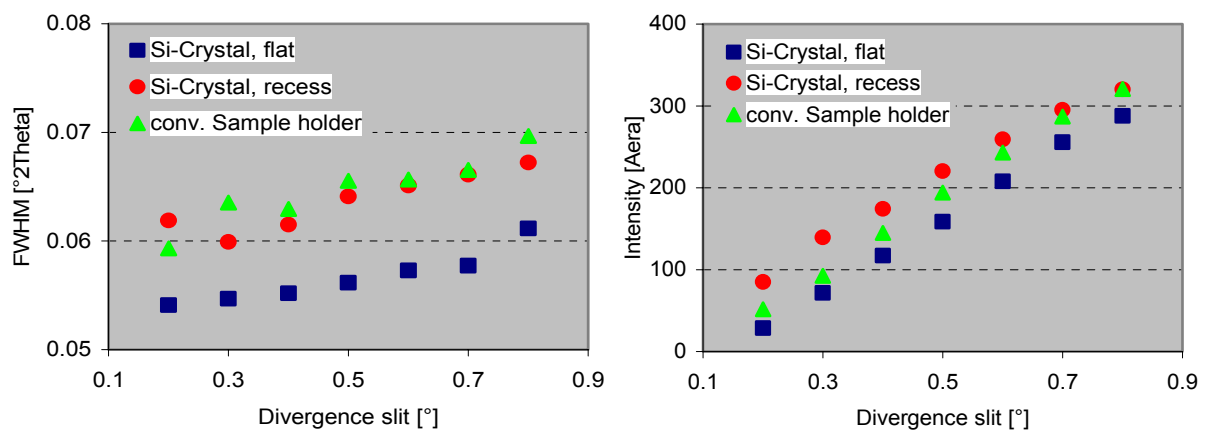


Fig. 3: FWHM (left) and intensity (right) of quartz peaks (100) and (101) in dependence of sample holder and divergence slit width

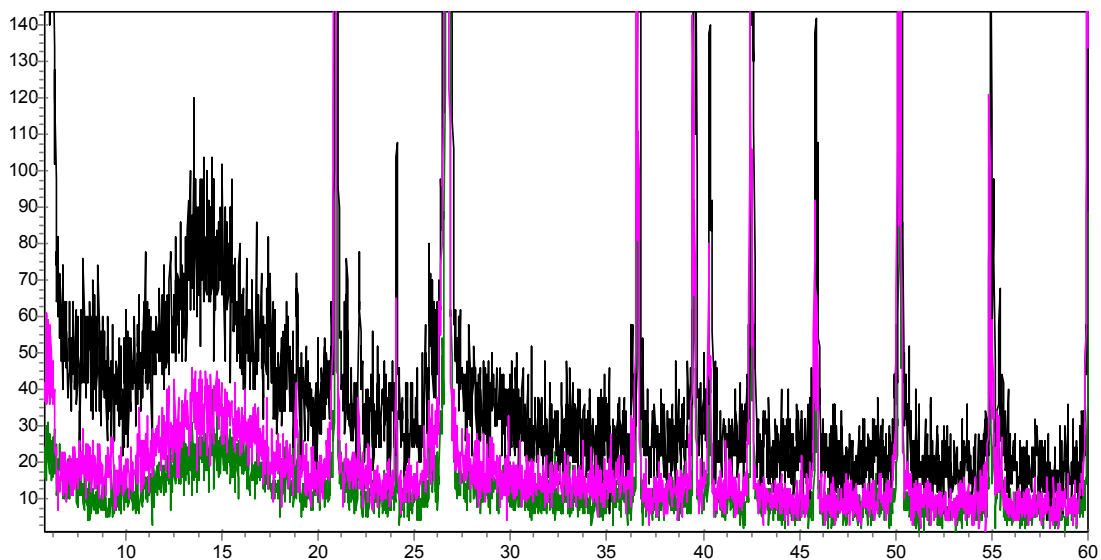


Fig. 4: Underground measured with conventional (black) and recessed single crystal sample holder (magenta) with tube voltage of 40 KV, conventional sample holder with 30 KV (green)

Reproducibility of standard measurements

Average peak widths (FWHM) obtained by fit and standard deviations of measurements X20-X48 are summarized in Tab. 3. The coarse RS-RDX C1 revealed no reproducible peak profiles when measured with the recessed silicon sample holder. With the oddly shaped profiles (Fig. 5, left) peak widths are very large, up to $0.25^\circ 2\theta$, and standard deviations are in the same order. Using the flat sample holder peaks become smooth suitable for a peak fit, and even intensities increase in spite of the reduced sample quantity (Fig. 5, right). Thus standard deviations slow down significantly. However, different preparation procedures delivered systematic deviations of peak widths, expressed by the different values of columns “same sample” (Series 2) and “refined preparation” in Tab. 3 and the outstanding run of the orange curve in Fig. 5 measured with a “thick” particle layer” (X34).

Measurements of fine RS-RDX C5 with the recessed sample holder delivered reasonable standard deviations, but large peak widths of $0.12^\circ 2\theta$ due to the low absorption of the RDX. By changing to the flat sample holder peak widths are significantly reduced, but standard deviation may increase as the preparation of a defined particle layer with constant thickness is difficult. However, the investigations show that a combination of high resolution and high reproducibility is reachable, as shown in column “refined preparation”.

Tab. 3: Mean peak widths and standard deviations in dependence of sample preparation techniques

RS-RDX		Peak	Ø FWHM and standard deviations (in brackets)		
Class	Holder		All samples*	same sample	Refined prep.
C1	recess	(111)	0.241(144)	0.101(148)	--
		(200)	0.219(130)	0.219(124)	--
	flat	(111)	0.094(21)	0.116(2)	0.072(2)
		(200)	0.075(30)	0.086(8)	0.049(9)
C5	recess	(111)	0.119(4)	0.117(1)	--
		(200)	0.122(4)	0.122(2)	--
	flat	(111)	0.076(11)	0.087(2)	0.065(3)
		(200)	0.072(14)	0.083(3)	0.062(13)

*except X34 and X48

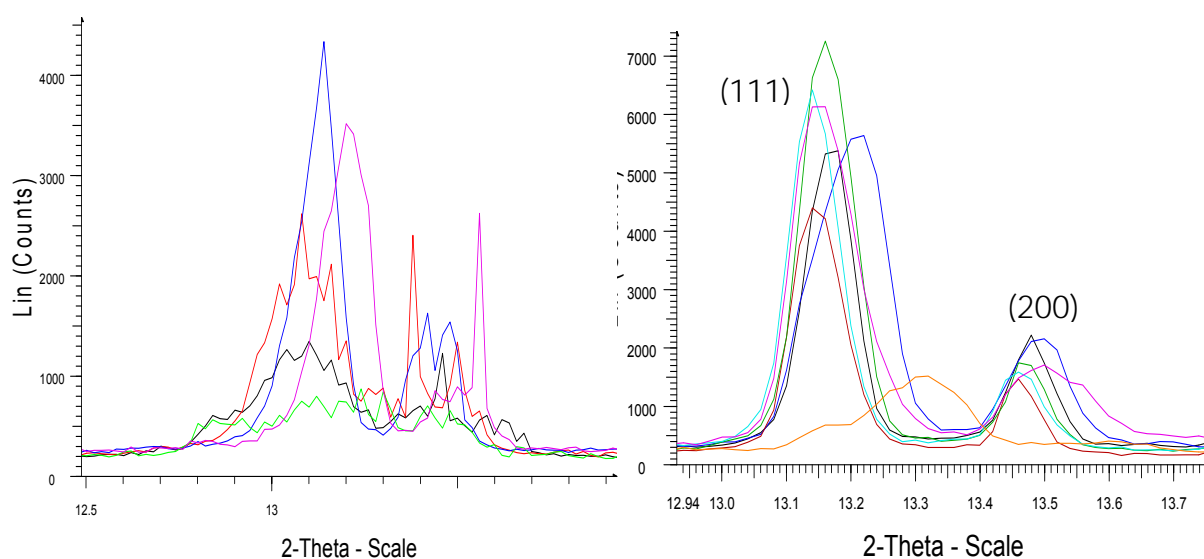


Fig. 5: Patterns of coarse RDX measured with recessed (left) and flat silicon sample holder (right)

Standard measurements of RDX, RS-RDX and I-RDX

Fig. 6 shows a comparison of the coarse samples RDX C1 (blue), RS-RDX C1 (red) and I-RDX C1 (green) measured with the recessed sample holder. The patterns give a first characterization of the materials, showing that reflexes from separated domains superpose to jagged intensities curves. The effect seems to be more pronounced with the I-RDX and RS-RDX compared to RDX; quantification, however, is difficult within the standard measuring technique. A reasonable determination of peak widths and a subsequent evaluation according to Williamson and Hall were not possible with these diffraction patterns.

Preparing the class 1 samples as thin particle layers delivered more smooth diffraction peaks suitable for peak fit and subsequent Williamson Hall plot. The evaluation, however, yielded widely distributed reciprocal peak widths between 0.0 and 0.05 $1/\text{\AA}$. No systematic curve or differences between samples could be recognized.

With the fine samples runs of Williamson Hall curves became clearer. Fig. 7 and Fig. 8 show the plots obtained with recessed sample holder (X57, X36, X36, X59) and thin particle layer (X10, X11, X13, X40, X41, X50, X58). The reciprocal peak widths measured with the recessed sample holder range from 0.3 to 0.8. Linear regression lines delivered slopes of 0.045, 0.83 and 0.1 for RDX, RS-RDX and I-RDX, respectively. Preparing the samples as thin particle layers reduced the reciprocal peak widths to 0.01 till 0.04. The slopes differ more significantly with values of -0.005, 0.045 and 0.083 for RS-RDX, I-RDX and RDX, respectively. It was found, however, that curves from different measuring series differ significantly and systematically; peak widths and slopes in the Williamson Hall plot were higher for series 1 (X10, X11, X13) than for series 2 (X40, X50, X58).

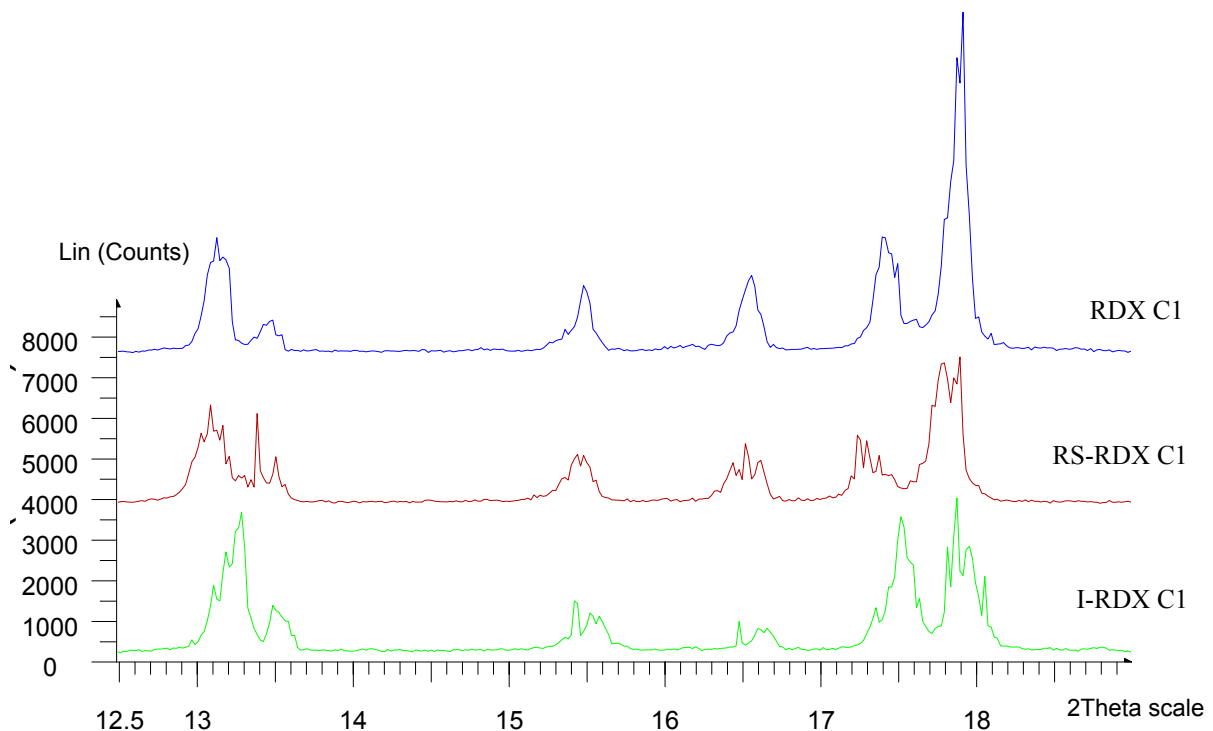


Fig. 6: Part of diffraction patterns of coarse RDX (class 1) measured with recessed sample holder

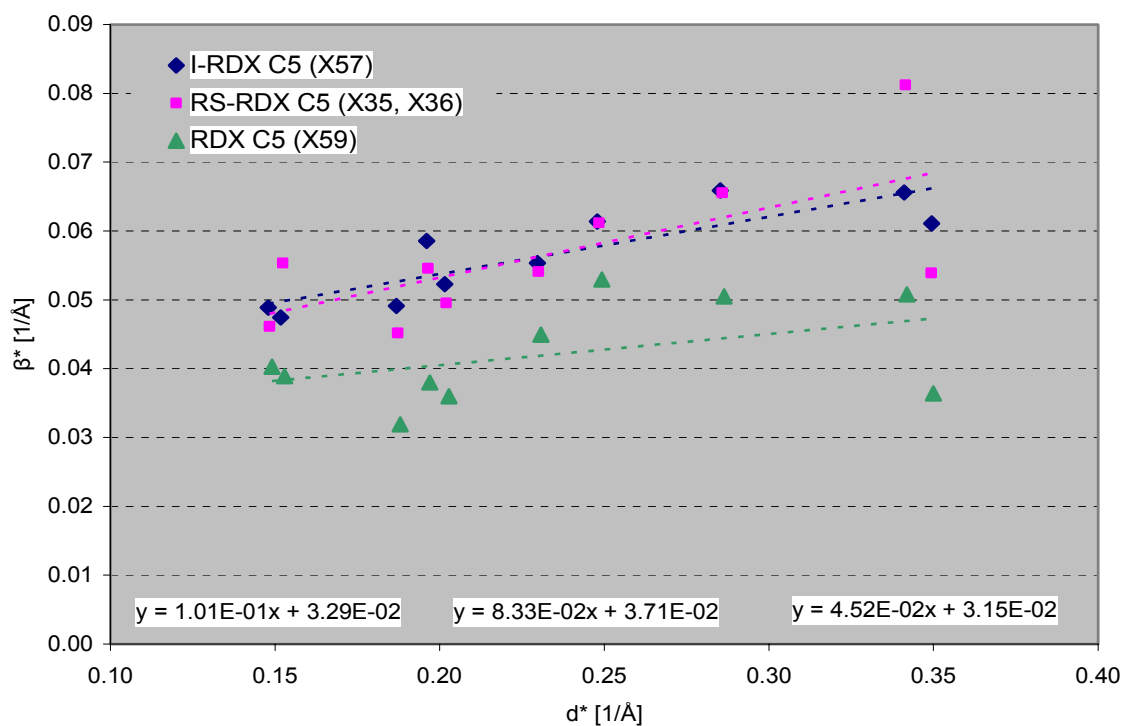


Fig. 7: Williamson Hall plot of conventional and reduced sensitivity RDX, class 5; measured with recessed sample holder

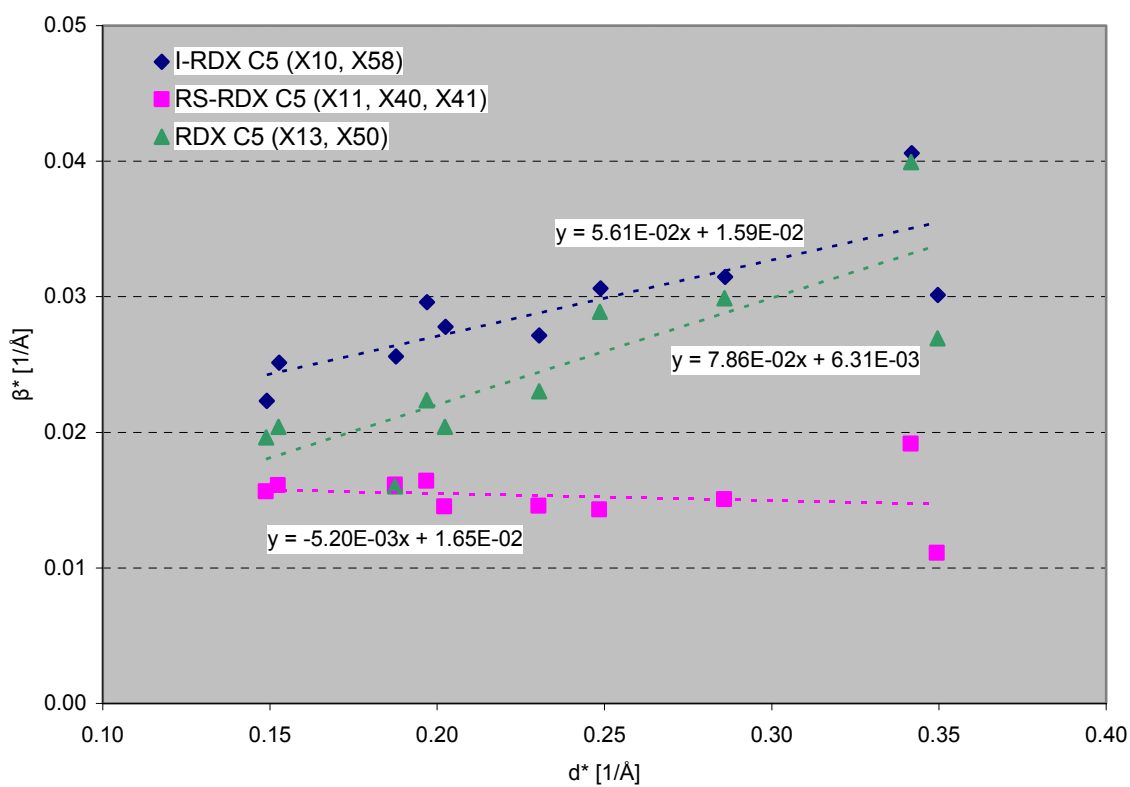


Fig. 8: Williamson Hall plot of conventional and reduced sensitivity RDX, class 5; measured with thin particle layers

Rocking curves of RDX, RS-RDX and I-RDX

Fig. 9 shows for example parts of rocking curves of reflections (111), (200) and (002) measured with RS-RDX.

The patterns of (111) and (002) reflections - blue and black, respectively – involve large numbers of peaks, whereas the red (200) pattern involves few clear separated peaks. Distributions of FWHM obtained from all fit-able peaks were plotted as normalized additive number of peaks versus peak widths as shown in

Fig. 10 for reflection (111). The different runs of these curves point to different crystal qualities.

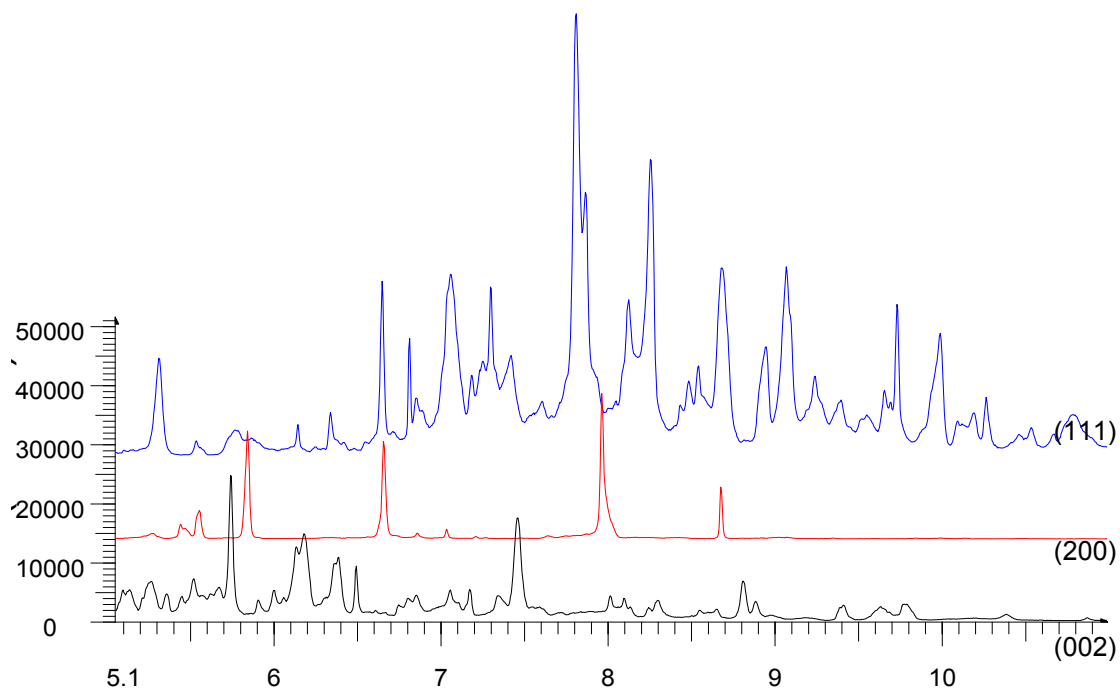


Fig. 9: Parts of rocking curves of (111), (200) and (020) reflections measured with RS-RDX

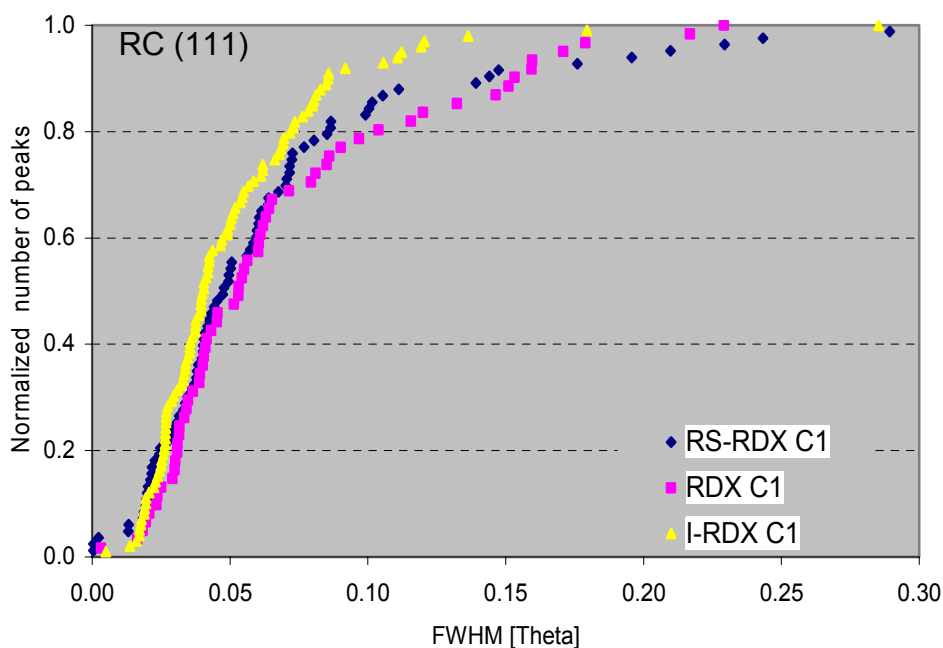


Fig. 10. Normalized additive number of peaks vs. peak width measured by rocking curves of reflection (111).

For quantifying the differences, mean peak widths (\O FWHM), median peak widths (X_{50}) and quotients X_{25}/X_{75} are summarized in Tab. 4. Values in brackets give standard deviations calculated from five repeated measurements with RS-RDX (X59-X63). Lowest mean and median peak widths are found for I-RDX with 0.044 and 0.033 followed by 0.067 and 0.047 for RS-RDX and 0,086 and 0,063 theta for RDX. Considering standard deviation of mean and median peak width around 0.011 and 0.006, respectively, the differences between RDX, RS-RDX and I-RDX are more than significant.

Tab. 4: Characteristic data of peak widths of coarse RDX samples obtained by rocking curves

Peak	RS-RDX (X59-X63)			I-RDX (X66+X67)			RDX (X64+X65)		
	\O FWHM	X_{50}	X_{25}/X_{75}	\O FWHM	X_{50}	X_{25}/X_{75}	\O FWHM	X_{50}	X_{25}/X_{75}
(111)	0.071(3)*	0.052(3)	0.43(4)	0.045	0.034	0.47	0.071	0.058	0.42
(200)	0.064(14)	0.038(6)	0.34(8)	0.045	0.032	0.51	0.080	0.058	0.53
(022)	0.061(6)	0.048(7)	0.46(5)	0.050	0.038	0.52	0.088	0.069	0.48
(220)	0.074(13)	0.054(7)	0.35(4)	0.037	0.030	0.54	0.121	0.077	0.35
(131)	0.064(17)	0.042(7)	0.44(7)	0.040	0.030	0.55	0.071	0.052	0.45
Gesamt	0.067(11)	0.047(6)	0.40	0.044	0.033	0.52	0.086	0.063	0.45

* Values in brackets give standard deviations in terms of last digit of related value

Discussion and comparison with Synchrotron data

Techniques

The measurements of coarse samples with standard techniques revealed jagged intensities curves. The jagged profiles stem from poor orientation statistics and high penetration depth, where shifted reflexes from few arbitrary domains superpose randomly. A reasonable evaluation of these profiles by means of peak fit was not possible. Thus this technique failed quantifying internal crystal quality of coarse RDX (class 1). But the degree of jaggedness and separation may give raw information about crystal quality. Preparing the coarse samples as thin particle layers improves the situation, in so far as profiles became smooth, suitable for peak fit. This was not expected, as with the smaller sample quantity of the thin layer orientation statistics should become even worse. A reduction of peak shift e.g. in Fig. 5 alone doesn't explain the effect. Secondary extinction and/or masking of particles one another may also influence the peak shapes.

The lack of poor orientation statistics of the coarse samples could be inverted into an advantage, when reflections from isolated domains could be evaluated separately. Within rocking curves domains are tilted in and out of reflection conditions, randomly. Evaluation of a large number of by this way monitored crystal domains delivers a representative characterization of coarse powders. The method is very promising, as applicable for as-crystallized products, where the old problem of deciding whether samples should be grinded to suitable size or crystal quality shouldn't be changed is overcome.

With the fine material, the lack of poor orientation statistics doesn't occur, but peak broadening due to high penetration depth is an issue. Preparing samples as a thin particle layer reduces penetration depths mechanically, but the already makeshift preparation of a homogenous layer with defined and controlled layer is difficult and has to be refined. However, measuring lowly absorbing materials as RDX prepared as thin layers carves out characteristic peak broadening more clearly.

A further advantage delivers parallel beam geometry, e.g. available at the synchrotron (ANKA). With the longer distances from source to sample and sample to detector, the higher intensity and resolution and geometric optics broadening due to penetration depth, mean density or uneven sample surface is strongly reduced or doesn't occur. Thus, measurements deliver a much better reproducibility. Fig. 11 shows e.g. a Williamson Hall plot of three HMX qualities, where results of same qualities (HMX 2 and HMX 2') are almost congruent.

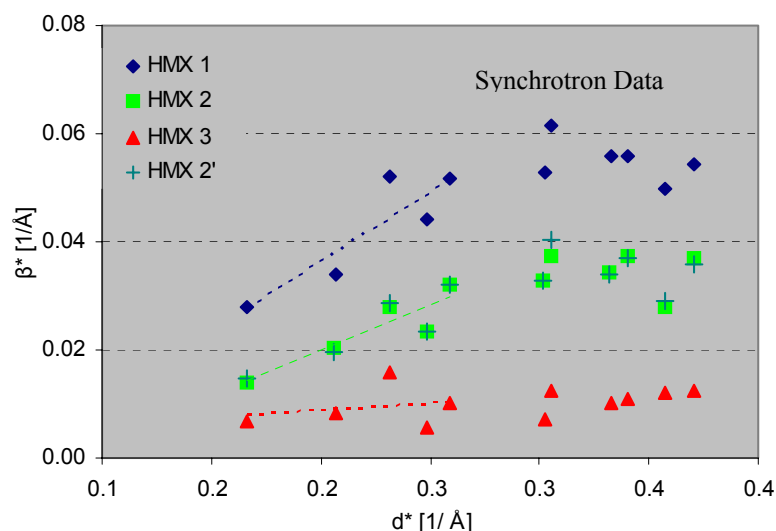


Fig. 11: Williamson Hall Plot of HMX qualities; high reproducibility of synchrotron data (HMX 2, HMX 2').

RDX, RS-RDX and I-RDX

The investigation of the fine RDX samples with the laboratory X-ray equipment using thin layer technique revealed significantly different plots. The slopes of the Williamson Hall in Fig. 8 point to a comparably low micro strain in I-RDX followed by RS-RDX and last conventional RDX. While the results are not yet quite confident - due to the makeshift preparation technique - results from synchrotron radiation give evidence on distinguishable RDX qualities in terms of peak broadening. Fig. 12 shows a Williamson Hall plot of the RDX qualities measured with synchrotron radiation. The plot shows significant differences between the conventional and the reduced sensitivity and insensitive RDX. Interpreting initial slope of the curves as a measure of micro strain, the plot would also point to lower micro strain in I-RDX and RS-RDX compared to the conventional RDX.

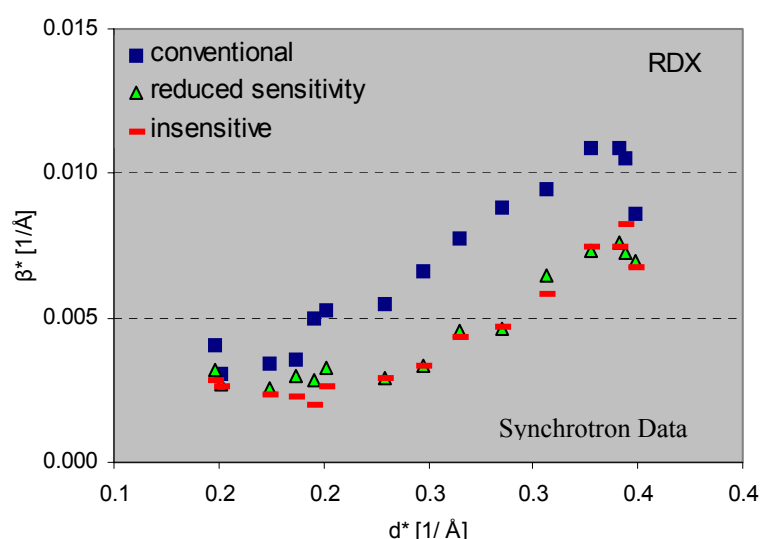


Fig. 12: Williamson Hall plot of RDX qualities, obtained by synchrotron investigations; Plot distinguishes conventional from RS- and I-RDX; cass 5.

A first hint on internal crystal quality of the coarse powders was found with the standard measurements, where jagged peaks occur in the diffraction patterns. The jaggedness seems to be more pronounced in patterns of I-RDX and RS-RDX compared to RDX, which may be interpreted as poorer

orientation statistics combined with smaller reflections representing higher crystal qualities. The effect, however, could not be quantified easily with the strongly superposing reflections. Measuring this effect with rocking curves delivers mean and median peak widths that definitely distinguish the different crystal qualities of the RDX samples. The higher widths of RDX compared to RS-RDX and I-RDX shown in Fig. 13 for different reflections, indicate a poorer crystal quality of the coarse conventional RDX compared to the RS- and I-RDX.

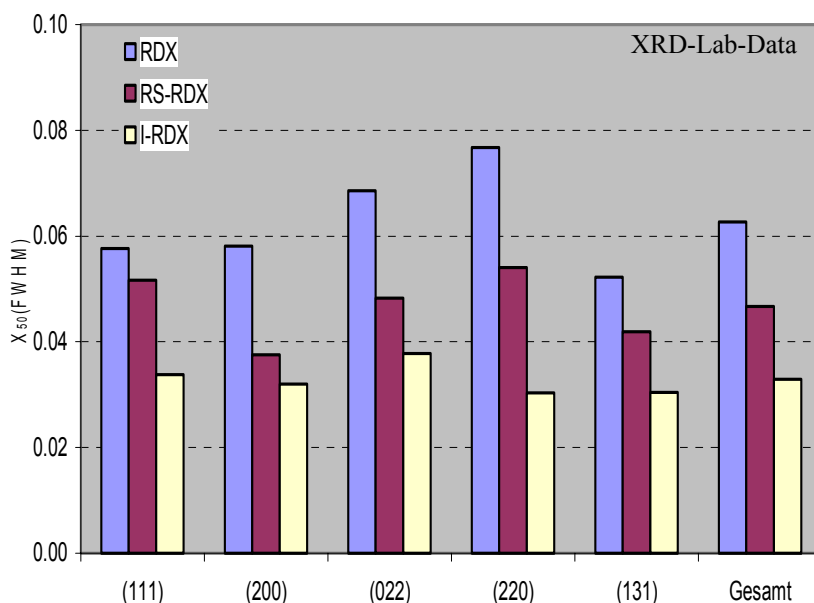


Fig. 13: Median peak widths obtained from rocking curves; plot distinguishes conventional from RS- and I-RDX, class 1. (Data from Tab. 4)

The refined or new X-ray diffraction techniques deliver powerful tools for the characterization and quality assessment of reduced sensitivity energetic materials. Insensitive and Reduced Sensitivity RDX have been significantly distinguished from conventional RDX. The results shall be discussed in terms of micro structure (size, strain) and support development and quality assessment of reduced sensitivity product.

References

- Armstrong RW, Ammon HL, Du ZY, Elban WL, Zhang XJ (1993) Mat Res Soc Symp Proc Vol 296, ISBN 1-55899-191-3
- Choi CS, Prince E (1972) Acta Cryst. B28, 2857-2862
- NIMIC (2003) Proc. of Reduced Sensitivity RDX Technical Meeting; November 2003, Meppen, Germany
- National Institute of Standards and Technology NIST (2000) Certificate of Standard Reference Material 660a, Gaithersburg, MD 20899
- Herrmann M (2003) Report European Office of Aerospace Research and Development, Contract number FA8655-02-M-4066
- Herrmann M, Fietzek H (2005) Powder Diffraction 20 (2), June 2005, 105-108
- Herrmann M (2005) Annual Report 2005; ANKA Synchrotron Radiation Facility for Microfabrication and Analytical Services; p 28 – 29

Klug PK, Alexander LE (1974) X-ray Diffraction Procedures for Polycrystalline and Amorphous Materials, Wiley, ISBN 0-471-49369-4

Schneider J.R. (1974) J. Appl. Cryst.7, 547-554

Spieß L, Schwarzer R, Behnken H, Teichert G (2005) Moderne Röntgenbeugung, BG Teubner Verlag, Wiesbaden, ISBN 3-519-00522-0

Ungár T (2000) in: Chung FH, Smith DK (2000) Industrial Applications of X-ray Diffraction; Marcel Dekker, Inc. New York, ISBN: 0-8247-1992-1

Warren BE, Averbach BL (1950) J Appl Phys Vol 21, 595-599

Yazici R, Mayo W, Takemoto T, Weissmann S (1983) J. Appl. Cryst. (1983) 16, 89-95

Acknowledgement

This material is based upon work supported by the European Office of Aerospace Research and Development, Air Force Office of Scientific Research, Air Force Research Laboratory, under Contract No. FA8655-05-1-3029.

Any opinion, findings and conclusions or recommendations expressed in this material are those of the authors and do not necessarily reflect the view of the European Office of Aerospace Research and Development, Air Force Office of Scientific Research, Air Force Research Laboratory.

Appendix

Tab 5: Diffraction measurements and conditions

ID	Sample	Sample Holder	2 θ / Step / Time [°] / [°] / [s]	Slits / Spinning div / det / [rpm]	Comments		
System check							
X1	Quartz	Standard	20.35-21.35; 26.15-27.15 / 0.002 / 6	0.1, 0.2, 0.3, 0.4, 0.5, 0.6, 0.7, 0.8 / 0.1 / 30	Slit and sample holder check		
X2		SC, recess					
X3		Flat SC					
X4		Standard	5-60 / 0.02 / 2	0.5 / 0.1 / 30 (Voltage 30 kV)	Voltage and sample holder check		
X5		SC, recess					
X6		flat SC					
X7		Standard		0.5 / 0.1 / 30 (Voltage 40 kV)			
X8		SC, recess					
X9		Flat SC					
Preliminary RDX series							
X10	I-RDX M3C	Flat SC	12.5-33 / 0.005 / 6	0,5 / 0.1 / 30	Series 0		
X11	RS-RDX C5						
X12	I-RDX-C1						
X13	RDX C5						
X14	RDX C1						
X15	RS-RDX C1						
Standard							
X16	SRM 660a	Flat SC	12-32 / 0.02 / 10s	0.5 / 0.1 / 30	Size/Strain-Standard		
X17		SC, recess					
X18		Flat SC	30-31 / 0.005 / 10s				
X19		SC, recess					
Reproducibility							
X20	RS-RDX C1	SC, recess	12-32 / 0.02 / 10s	0.5 / 0.1 / 30	Series 1		
X21 - X24		Flat SC			12-32 / 0.02 / 10s	0.5 / 0.1 / 30	Series 2: same sample stirred
X25							Series 1
X26 - X29							Series 2: same sample stirred
X30 - X32							Series 3: preparation check
X33							S3 small quantity
X34	S3 large quantity						
X35	RS-RDX C5	SC, recess	12-32/0.02 10s	0.5 / 0.1 / 30	Series 1		
X36 - X39		Flat SC			12-32/0.02 10s	0.5 / 0.1 / 30	Series 2: same sample stirred
X40							Series 1
X41 - X44							Series 2: same sample stirred
X45 -X46							Series 3: preparation check
X47							S3 small quantity
X48	S3 large quantity						
RDX series							
X20	RS-RDX C1	SC, recess	12-32/0.02 10s	0.5 / 0.1 / 30	Series 1		
X35	RS-RDX C5						
X49	RDX C5					Flat SC	
X50		SC, recess					
X51	RDX C1	Flat SC					
X52		SC, recess					
X53 - X54	I-RDX C1	Flat SC					
X55		SC, recess					
X56		Flat SC					
X57	I-RDX M3C	SC, recess					
X58		Flat SC					
Rocking Curves			2 θ / θ / Step / Time				
X59 - X63	RS-RDX C1	Flat SC	13.169 / 1.585-11.585 13.507 / 1.753-11.753	0.5 / 0.1 / 30	Series RC + reproducibility check		
X64 - X65	RDX C1		16.589 / 3.295-13.295 20.475 / 5.237-15.237		Series RC		
X66- X67	I-RDX C1		25.465 / 7.733-17.733 0.005 / 6s				

Abbr.: SC = Single Crystal sample holder, RC = Rocking Curve; Tube, 40 kV, 40 mA (if not defined else)

(1) 19.808 / 4.904-14.904 instead of 20.475 / 5.237-15.237 for X59